Chemistry–A European Journal
Research Article
doi.org/10.1002/chem.202200538
Chemistry Europe
European Chemical Societies Publishing
www.chemeurj.org

Generalizing the Aromatic δ-Amino Acid Foldamer Helix

Daniel Bindl,[a] Pradeep K. Mandal,[a] and Ivan Huc*[a]

Abstract: A series of aromatic oligoamide foldamer sequences containing different proportions of three δ-amino acids derived from quinoline, pyridine, and benzene and possessing varying flexibility, for example due to methylene bridges, were synthesized. Crystallographic structures of two key sequences and ^{1}H NMR data in water concur to show that a canonical aromatic helix fold prevails in almost all cases and that helix stability critically depends on the ratio between rigid and flexible units. Notwithstanding subtle variations of curvature, i.e. the numbers of units per turn, the aromatic δ-peptide helix is therefore shown to be general and tolerant of a great number of sp^3 centers. We also demonstrate canonical helical folding upon alternating two monomers that do not promote folding when taken separately: folding occurs with two methylenes between every other unit, not with one methylene between every unit. These findings highlight that a fine-tuning of helix handedness inversion kinetics, curvature, and side chain positioning in aromatic δ-peptidic foldamers can be realized by systematically combining different yet compatible δ-amino acids.

Introduction

Folding is an essential mechanism used by nature to achieve a wide variety of sophisticated, structurally precise architectures and functions, in particular in proteins.[1] Foldamers are artificial molecules based on non-natural backbones or sequences that also have the ability to fold in a well-defined way, with helical and sheet-like structures being prevalent motifs.[2] Canonical aromatic helices have become a major class of foldamer secondary motifs. They comprise main chain aryl rings that stack upon helix folding, therefore defining a vertical rise per turn, or pitch, equal to the thickness of an aromatic unit (ca. 3.5 Å). A wide range of backbone types adopt aromatic helical conformations, including phenylene-ethynylenes,[3] aryl-aryl linked backbones,[4] aryl hydrazones,[5] aryl ureas,[6] and aryl amides.[7] Depending on the backbone, different forces may contribute to aromatic helix stability, most notably hydrogen bonds and electrostatic repulsions between contiguous units, as well as interactions associated with aromatic stacking such as solvophobic effects. Main chain aromatic units endow aromatic helices with distinct properties and functionalities compared to α-peptidic structures and their homologs,[8] for example structural predictability,[9] generally high conformational stability, photophysical properties,[10] charge transport ability[11] or the possibility to create a cavity within a single helical conformation for guest encapsulation.[12]

Aromatic amide foldamers are of particular interest because of their easy synthetic access and amenability to solid-phase synthesis. Oligoamides of δ-amino acid 8-aminoquinoline-2-carboxylic acid (Q) fold into stable aromatic helices in essentially all solvents (Figure 1).[13] In this backbone, amide and aryl groups exclusively consist of sp^2 centers, enabling a high degree of π-stacking in the Q_n helix. Intramolecular hydrogen bonding pinches the main chain leading to a high curvature of five units per two turns. Therefore, when looking down the helix axis, the helix wheel looks like a five-pointed star (Figure 1c). Positions 4, 5, and 6 of Q may be functionalized by

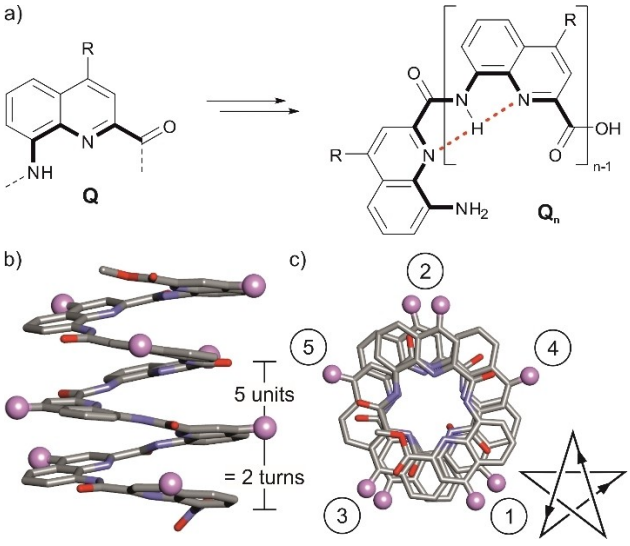

Figure 1. a) Structure of Q and its oligomer. Hydrogen bonds on the inner rim of the helix are indicated as red dashed lines. Crystal structure of a Q_8 oligomer,[17] representative of the canonical aromatic helix fold, in side (b) and top (c) view. Only the first atom of R side chains is shown as a purple ball to indicate their positions, and hydrogen atoms are omitted for clarity.

[a] D. Bindl, Dr. P. K. Mandal, Prof. I. Huc
Department of Pharmacy and Center for Integrated Protein Science
Ludwig-Maximilians-Universität
Butenandtstraße 5–13, München 81377 (Germany)
E-mail: ivan.huc@cup.lmu.de

Supporting information for this article is available on the WWW under https://doi.org/10.1002/chem.202200538

side chains that will diverge from the Q_n helix for the purpose of molecular recognition at the helix surface.[14] The question that we addressed in the present study is the generality of the folding pattern of Q_n oligomers. Other than Q, aromatic δ-amino acids 6-(aminomethyl)pyridine-2-carboxylic acid (P)[15] and 2-(2-aminophenoxy)acetic acid (B)[16] have been introduced (Figure 2a). P and B correspond to a Q in which the benzene or the pyridine ring has been deleted, respectively, while preserving a hydrogen bond acceptor as a main chain atom, namely the endocyclic nitrogen atom of P and the ether oxygen atom of B. P and B, each possess a reduced surface for aromatic stacking, thus reduced hydrophobicity, as well as one sp^3 center and additional rotatable bonds conducive of enhanced flexibility. In the following, we generalize the compatibility of B, P, and Q units to form canonical aromatic helices in water. We show that a single Q may significantly enhance helix stability. We also report an intriguing sequence dependence, in that a $(PB)_n$ oligomer folds in the absence of any Q unit, whereas P-only or B-only sequences do not.

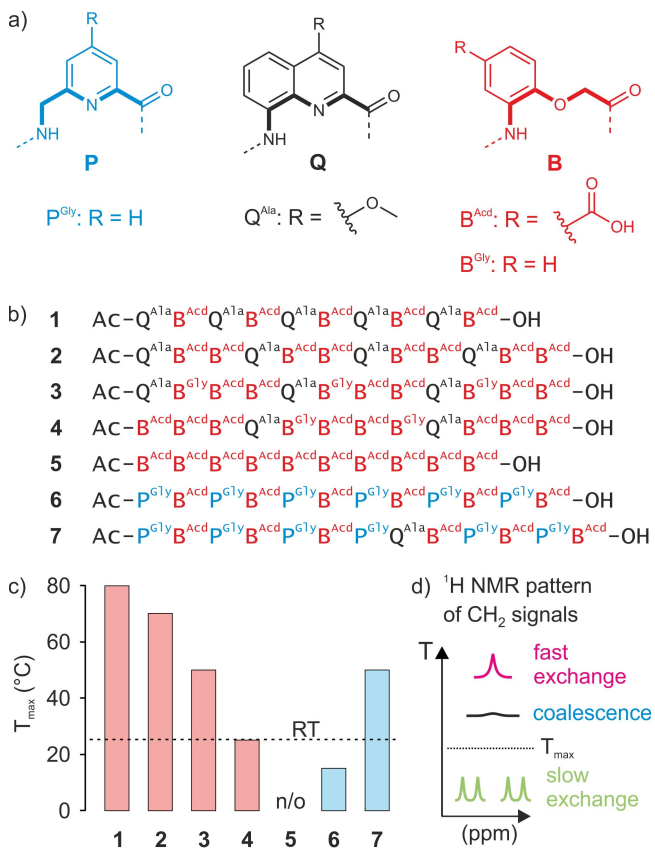

Figure 2. a) Structures of the building blocks used in this study. The different types of monomer structures and letter codes are indicated by different colors. b) Sequences that were investigated in this study. c) Comparison of T_{max} of anisochronicity for **1**–**7**. n/o: not observed d) Definition of T_{max} as the highest temperature at which anisochronous signals were clearly observed for methylene groups by ^{1}H NMR (for compound **1**, coalescence was not reached at 80 °C). Sequences without P are represented by red bars, while sequences with P are shown in blue. Room temperature (RT = 25 °C) is indicated with a dashed line.

Results and Discussion

The additional flexibility of P and B was previously shown to be detrimental to canonical aromatic helix folding. Specifically, the main chain methylene groups were found to promote 90° kinks. These kinks may be disruptive of folding – P_n oligomers fold neither in chloroform[15a] nor in water.[15b] They may also promote different, non-canonical, folding modes – a B_n oligomer formed a so-called herringbone helix in the solid state.[16a] The more rigid Q units have been shown to template the formation of canonical aromatic helices containing otherwise flexible monomers.[18] However, $(PQ)_n$ was also found to fold into a herringbone helix in chloroform,[15a] and to only adopt a canonical aromatic helix conformation in water.[15b] We thus began this investigation with the expectation that a large proportion of Q units may be necessary to stabilize aromatic helices, even in water. The following demonstrates that this is not the case. Instead, we show that B, P, and Q units can be generally mixed without losing the canonical aromatic helix fold in water.

Short side chains were used to preserve the naturally high crystal growth ability of aromatic foldamers.[14b] Q^{Ala} was chosen due to its easy synthetic accessibility, however, being non-polar, a solubilizing side chain was needed on the B units. New monomer B^{Acd} was prepared to promote solubility in neutral or basic aqueous medium. Starting from 4-hydroxy-3-nitrobenzaldehyde, a carboxylic acid was obtained through oxidation of the aldehyde and subsequently protected as a *tert*-butyl ester. The general route to Fmoc-protected B monomers described earlier could then be applied (Figure S1),[16b] and the final monomer was obtained in 26% overall yield over 5 steps. Oligomers **1**–**7** comprised of P^{Gly}, Q^{Ala}, B^{Gly}, and B^{Acd} monomers were then synthesized using low loading Wang or Cl-MPA ProTide™ resins (the latter is advantageous for the synthesis of sequences prone to aggregation) according to solid-phase foldamer synthesis (SPFS) protocols reported previously.[15b,19] Final products were purified by semi-preparative reversed-phase HPLC and were obtained in good overall yields (6.3–31%; section 2.2, Supporting Information).

Furthermore, downfield shifted amide signals indicate their involvement in intramolecular hydrogen bonding. Helix stability may also be assessed by ^{1}H NMR through the observation of helix handedness inversion kinetics. Since helices are chiral objects (present as a racemic mixture when the backbone contains no stereogenic center), methylene protons on the molecule are diastereotopic. As the magnetic environments above and below a given monomer differ due to different ring current effects, methylene protons that are close to the helix backbone often become anisochronous, i.e. have different ^{1}H NMR chemical shift values and appear as doublets notwithstanding other couplings. This holds only when *P*- and *M*-helical conformers exchange slowly on the NMR timescale. When the exchange is fast, averaged signals are observed as an indication of faster kinetics and weaker helix stability (yet not as an indication of helix unfolding). In Q_n oligomers, helix handedness kinetics vary with solvent polarity and with the value of n. Exceptionally long half-lives and even kinetic inertness have

been reported.[20] Heating enhances handedness inversion dynamics.[13]

With our first design, oligomer **1**, we aimed to test whether the templating effect observed for $(PQ)_n$ sequences in water[15b] is transferable to $(BQ)_n$ sequences, i.e. the ability of Q units to impose aromatic helix folding to more flexible B monomers. The ^{1}H NMR spectrum of **1** in aqueous solution has all the characteristics of an aromatic helix structure mentioned above (Figure 3). Diastereotopic signals (doublets) of the methylene groups of its B monomers in the area of 1.5–4.5 ppm indicate folding into a chiral conformation, of which the enantiomers exchange slowly on the NMR timescale. Upon heating to 80 °C (higher temperatures were not tested), anisochronicity remained indicating that kinetics of handedness inversion remained slow (Figure S2) and suggesting a very stable structure. An x-ray structure of **1** was obtained and confirmed the canonical aromatic helix fold (Figure 4a,b). The structure is similar to that of Q_n oligomers except for its curvature. In **1**, 2.33 units are needed to span one helix turn (instead of 2.5 in Q_n), and side chains are ordered in seven distinct arrays when looking down the helix axis instead of five (2.33 units per turn means 7 units for 3 turns). Since the B units contain sp^3 hybridized centers, some bond angles may differ from those of an all sp^2 backbone and thus alter the overall curvature as well as side chain positions. However, one may object that such an effect was not observed upon mixing Q and P even though the latter also contain methylene groups.[18a] Full structure elucidation in solution might allow for the assessment of these differences in solution but were not undertaken in the context of this study.[21] In any case, it can be concluded that Q units template the folding of B monomers as they do for P monomers.

The high stability of $(BQ)_n$ encouraged the investigation of "B_nQ_m" sequences, that is, oligomers containing n B and m Q units mixed throughout the sequence with a higher n/m ratio, to see how many Q units are necessary to keep the oligomers well-folded. Sequences **2**–**4** were thus prepared (Figure 2b). In these sequences, Q monomers were evenly distributed to ensure a homogeneous folding behavior. To prevent oligomers from carrying too many negative charges, which might bias the investigation by introducing possibly destabilizing electrostatic repulsions, B^{Acd} was replaced by B^{Gly} in some places. Remarkably, the ^{1}H NMR spectra of all sequences show an extensive chemical shift distribution of signals and slow exchange between *P*- and *M*-conformers (Figure 3). The similarity of these NMR spectra with that of **1** suggests that all fold into canonical aromatic helices in aqueous solution at room temperature. At least, it can be concluded that the templating effect of Q induces a well-folded structure in "B_nQ_m" oligomers, with an n/m ratio of up to 5/1. To estimate the stability of **2**–**4** in comparison to **1**, variable temperature studies were conducted (Figure S2–5). Oligomers **2**–**4** displayed coalescence of the diastereotopic signals in their ^{1}H NMR spectra at 80, 60, and 40 °C, respectively, which demonstrates a trend of decreasing stability when increasing the n/m ratio (Figure 2c). It is a significant observation that only two Q units in a 12-mer are sufficient to generate a stable well-folded structure.

The synthesis of an oligomer containing only one Q and multiple B units was attempted repeatedly. For unclear reasons, these attempts were not successful. One might invoke the conformational behavior of B-rich sequences in organic solvents during SPFS, i.e. possible aggregation. Yet, the all-B sequence **5** was successfully prepared. Its ^{1}H NMR spectrum showed clustering of signals in a few groups, implying reduced aromatic stacking (Figure 3). Some amide NH signals are broad and not downfield shifted and others have completely disappeared. This disappearance may reflect higher exposure of these protons to the solvent and exchange with water, which would result in some signal suppression. Such a phenomenon would clearly indicate a loss of the aromatic helical structure in which amide

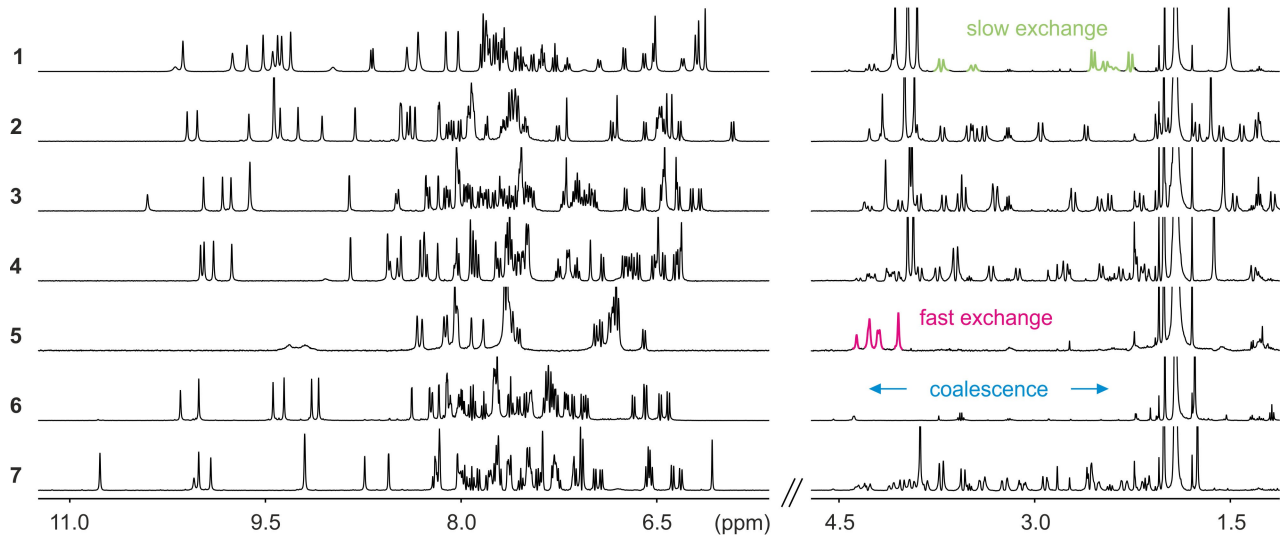

Figure 3. ^{1}H NMR spectra of compounds **1**–**7** (500 MHz, 12 mM NH_4OAc buffer pH 8.5 with 10% D_2O, water suppression). Anisochronous signals of diastereotopic methylene protons are highlighted in green exemplary in the spectrum of **1**. Singlets of methylene groups are highlighted in purple in spectrum of **5**.

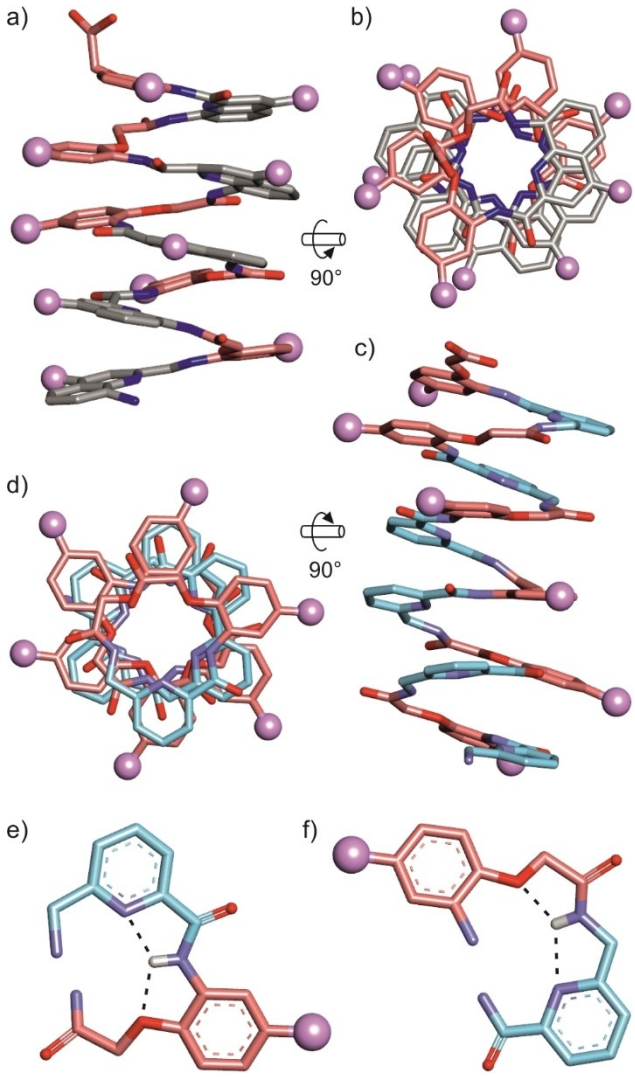

Figure 4. Crystal structure of **1** in side (a) and top (b) view. Crystal structure of **6** in side (c) and top (d) view. Q, B, and P monomers are shown in gray, red, and blue, respectively. Only the first atom of side chains is shown as a purple ball to indicate their positions, and hydrogen atoms are omitted for clarity. e, f) Parts of the crystal structure of **6** illustrating the rigid part between P and B (e) and the extended flexible part between B and P (f). Amide hydrogen atoms are shown, and hydrogen bonding is indicated with black dashed lines.

protons are normally buried in the helix channel. Furthermore, sequence **5** does not display diastereotopic doublets for its methylene groups (singlets are observed) even at 0 °C (Figure 2c, S6), meaning that its conformation is either achiral or that the exchange between different chiral folded states is fast on the NMR time scale. We could not obtain crystals of **5** and the exact nature of B_n oligomer conformations in aqueous solution remains unclear. It can only be concluded that at least some Q units are necessary to template B units into the canonical aromatic helix fold.

As stated above, oligomers only comprised of P units also do not fold into well-defined structures in aqueous media.[15b] However, these findings cannot be extrapolated to molecules of the type "B_nP_m", since they contain different flexible and rigid parts than either only B or P containing sequences. "B_nP_m" oligomers comprise an extended flat and rigid aromatic dimer when a B unit follows P and a long flexible -$OCH_2CONHCH_2$- linkage when P follows B (Figure 4e,f). To investigate the effects of mixing B and P monomers on folding behavior, sequence **6** was designed, which consists of an alternation of B and P units. Like compounds **1**–**4**, oligomer **6** shows again widespread ^{1}H NMR signals and downfield shifted amide signals (Figure 3). This indicates both more extensive aromatic stacking and stronger intramolecular hydrogen bonding in **6** compared to **5**. In fact, the ^{1}H NMR spectrum of **6** resembles more those of Q-containing sequences **1**–**4** than that of **5**. However, it does not show diastereotopic signals in the aliphatic region. The methylene signals are very broad to invisible, suggesting coalescence is reached at room temperature. Upon cooling to 0 °C the signals split into doublets, demonstrating that well-defined folded states with slow exchange on the NMR timescale can be obtained with a "B_nP_m" sequence at lower temperatures (Figure 2c, S7). An x-ray structure of **6** could be obtained, which confirmed a canonical aromatic helix fold, despite the lack of any Q units and the long flexible linkages between B and P monomers (Figure 4c-f). Again, a curvature change compared to Q_n oligomers can be observed. In the case of **6**, 2.4 units are necessary to propagate the helix by one turn (amounting to 12 units for 5 turns). Side chain positioning is altered as well.

Given that **6** is the least stable folded oligomer investigated in this study (lowest T_{max} of observable anisochronous methylene signals), its canonical fold in the solid state suggests that the aromatic helix also prevails in **2**–**4** for which no crystal structure could be obtained. These results provide evidence that the rigid PB dimers counteract the flexibility of the BP linkage. In other words, the aromatic helix is more tolerant towards larger aromatic units (PB) and more flexible BP linkages than to smaller aromatic units (P or B) separated by less flexible but twice more numerous linkages containing sp^3 centers. The stability of "B_nP_n" oligomers, with equal numbers of B and P units, is thus dependent not only on n but also on the sequence. One can speculate that $(PB)_n$ should be the most stable (note that compound **6** is $(BP)_6$) and B_nP_n the least stable since it does not have any PB combination.

Finally, we aimed to test whether the stabilizing effect of Q units seen for "B_nQ_m" can be extended to "B_nP_m" oligomers. For this purpose, sequence **7** with an additional Q monomer compared to **6** was synthesized. The Q unit was placed in such a manner that it enlarges the flat, rigid part between one P and one B. The ^{1}H NMR signals of **7** expectedly indicate canonical folding. Methylene signals appear as doublets at room temperature (Figure 3) and up to 60 °C (Figure 2c, S8). This stability is comparable to that of "B_9Q_3" (i.e. **3**), which again illustrates the increased stability of $(PB)_n$ as opposed to B-only sequences: 1 vs. 3 Q units are needed for the same T_{max} of anisochronicity. It can be assumed that introducing additional Q units within "B_nP_m" sequences would further enhance stability as it did in **1**–**4**.

Conclusion

In conclusion, it was shown that B, P, and Q units are essentially interchangeable in helical aromatic δ-amino acid foldamers. "B_nQ_m" oligomers, with an n/m ratio of up to 5/1 still fold into canonical helices. Their stability decreases as n/m increases but appears to remain above that of most aliphatic peptidic helices for which slow exchange of helix handedness inversion on the NMR timescale has rarely been observed.[22] Sequences with alternating B and P units possess an increased folding propensity compared to only B- or P-containing oligomers, and fold into a canonical aromatic helix even without any Q unit within their sequence, albeit cooling was required for $(PB)_6$ to display slow handedness exchange on the NMR timescale. Significant stabilization of $(PB)_6$ was achieved through introducing a single Q monomer within the sequence, leading to an increase of T_{max} of anisochronicity by 35 °C. Furthermore, the introduction of B monomers into Q-oligomers not only influences helix stability, but it also influences curvature and side chain positioning of the resulting foldamers, as shown by two different x-ray structures. Therefore, we demonstrated that adjusting the ratio and/or order of B, P, and Q allows for a fine-tuning of helix stability and side chain positioning without changing the overall fold. This ability will be useful in the context of molecular recognition at the helix surface, for example for foldamer-protein interactions.

Experimental Section

Deposition Numbers 2125508 (for **1**), 2125515 (for **6**) contain the supplementary crystallographic data for this paper. These data are provided free of charge by the joint Cambridge Crystallographic Data Centre and Fachinformationszentrum Karlsruhe Access Structures service.

Acknowledgements

This work was supported by the DFG (Excellence Cluster 114, CIPSM). We thank C. Douat for implementing automated solid phase synthesis. D. Gill is gratefully acknowledged for contributing synthetic precursors, and C. Glas for assistance with NMR measurements. We thank D. Staudacher for preliminary contributions to synthesis and crystallization experiments. Synchrotron data were collected at beamlines P13 and P14 operated by EMBL Hamburg at the PETRA III storage ring (DESY, Hamburg, Germany). We thank D. von Stetten and G. Bourenkov for their assistance in using the beamlines. Open Access funding enabled and organized by Projekt DEAL.

Conflict of Interest

The authors declare no conflict of interest.

Data Availability Statement

The crystallographic data that support the findings of this study are openly available from the Cambridge Crystallographic Data Centre at https://ccdc.cam.ac.uk, reference numbers 2125508 and 2125515.

Keywords: delta-peptides · foldamers · helical conformation · structure elucidation · x-ray crystallography

[1] C. M. Dobson, *Nature* **2003**, *426*, 884–890.
[2] a) S. H. Gellman, *Acc. Chem. Res.* **1998**, *31*, 173–180; b) D. J. Hill, M. J. Mio, R. B. Prince, T. S. Hughes, J. S. Moore, *Chem. Rev.* **2001**, *101*, 3893–4012; c) G. Guichard, I. Huc, *Chem. Commun.* **2011**, *47*, 5933.
[3] J. C. Nelson, *Science* **1997**, *277*, 1793–1796.
[4] a) D. M. Bassani, J.-M. Lehn, G. Baum, D. Fenske, *Angew. Chem. Int. Ed.* **1997**, *36*, 1845–1847; *Angew. Chem. Int. Ed.* **1997**, *109*, 1931–1933; b) M. S. Newman, D. Lednicer, *J. Am. Chem. Soc.* **1956**, *78*, 4765–4770.
[5] J.-L. Schmitt, A.-M. Stadler, N. Kyritsakas, J.-M. Lehn, *Helv. Chim. Acta* **2003**, *86*, 1598–1624.
[6] A. Tanatani, H. Kagechika, I. Azumaya, R. Fukutomi, Y. Ito, K. Yamaguchi, K. Shudo, *Tetrahedron Lett.* **1997**, *38*, 4425–4428.
[7] a) V. Berl, I. Huc, R. G. Khoury, M. J. Krische, J.-M. Lehn, *Nature* **2000**, *407*, 720–723; b) J. Zhu, R. D. Parra, H. Zeng, E. Skrzypczak-Jankun, X. C. Zeng, B. Gong, *J. Am. Chem. Soc.* **2000**, *122*, 4219–4220; c) Y. Hamuro, S. J. Geib, A. D. Hamilton, *J. Am. Chem. Soc.* **1996**, *118*, 7529–7541; d) A. Tanatani, A. Yokoyama, I. Azumaya, Y. Takakura, C. Mitsui, M. Shiro, M. Uchiyama, A. Muranaka, N. Kobayashi, T. Yokozawa, *J. Am. Chem. Soc.* **2005**, *127*, 8553–8561.
[8] a) D. H. Appella, L. A. Christianson, I. L. Karle, D. R. Powell, S. H. Gellman, *J. Am. Chem. Soc.* **1996**, *118*, 13071–13072; b) D. Seebach, M. Overhand, F. N. M. Kühnle, B. Martinoni, L. Oberer, U. Hommel, H. Widmer, *Helv. Chim. Acta* **1996**, *79*, 913–941; c) R. P. Cheng, S. H. Gellman, W. F. Degrado, *Chem. Rev.* **2001**, *101*, 3219–3232; d) D. Seebach, D. F. Hook, A. Glättli, *Biopolymers* **2006**, *84*, 23–37; e) M. D. Smith, T. D. W. Claridge, G. W. J. Fleet, G. E. Tranter, M. S. P. Sansom, *Chem. Commun.* **1998**, 2041–2042; f) H.-D. Arndt, B. Ziemer, U. Koert, *Org. Lett.* **2004**, *6*, 3269–3272; g) U. Koert, *J. Prakt. Chem.* **2000**, *342*, 325–333.
[9] I. Huc, *Eur. J. Org. Chem.* **2004**, *2004*, 17–29.
[10] a) D. Zheng, L. Zheng, C. Yu, Y. Zhan, Y. Wang, H. Jiang, *Org. Lett.* **2019**, *21*, 2555–2559; b) S. Pramanik, B. Kauffmann, S. Hecht, Y. Ferrand, I. Huc, *Chem. Commun.* **2021**, *57*, 93–96; c) A. M. Ortuño, P. Reiné, S. Resa, L. Alvarez De Cienfuegos, V. Blanco, J. M. Paredes, A. J. Mota, G. Mazzeo, S. Abbate, J. M. Ugalde, V. Mujica, G. Longhi, D. Miguel, J. M. Cuerva, *Org. Chem. Front.* **2021**, *8*, 5071–5086.
[11] a) A. Méndez-Ardoy, N. Markandeya, X. Li, Y.-T. Tsai, G. Pecastaings, T. Buffeteau, V. Maurizot, L. Muccioli, F. Castet, I. Huc, D. M. Bassani, *Chem. Sci.* **2017**, *8*, 7251–7257; b) L. Chen, Y.-H. Wang, B. He, H. Nie, R. Hu, F. Huang, A. Qin, X.-S. Zhou, Z. Zhao, B. Z. Tang, *Angew. Chem. Int. Ed.* **2015**, *54*, 4231–4235; *Angew. Chem.* **2015**, *127*, 4305–4309; c) J. Nejedlý, M. Šámal, J. Rybáček, M. Tobrmanová, F. Szydlo, C. Coudret, M. Neumeier, J. Vacek, J. Vacek Chocholoušová, M. Buděšínský, D. Šaman, L. Bednárová, L. Sieger, I. G. Stará, I. Starý, *Angew. Chem. Int. Ed.* **2017**, *56*, 5839–5843; *Angew. Chem. Int. Ed.* **2017**, *129*, 5933–5937.
[12] a) N. Chandramouli, Y. Ferrand, G. Lautrette, B. Kauffmann, C. D. Mackereth, M. Laguerre, D. Dubreuil, I. Huc, *Nat. Chem.* **2015**, *7*, 334–341; b) J. Garric, J.-M. Léger, I. Huc, *Chem. Eur. J.* **2007**, *13*, 8454–8462; c) W. Q. Ong, H. Zhao, X. Fang, S. Woen, F. Zhou, W. Yap, H. Su, S. F. Y. Li, H. Zeng, *Org. Lett.* **2011**, *13*, 3194–3197; d) R. B. Prince, S. A. Barnes, J. S. Moore, *J. Am. Chem. Soc.* **2000**, *122*, 2758–2762.
[13] H. Jiang, J.-M. Léger, C. Dolain, P. Guionneau, I. Huc, *Tetrahedron* **2003**, *59*, 8365–8374.
[14] a) M. Zwillinger, P. S. Reddy, B. Wicher, P. K. Mandal, M. Csékei, L. Fischer, A. Kotschy, I. Huc, *Chem. Eur. J.* **2020**, *26*, 17366–17370; b) X. Hu, S. J. Dawson, P. K. Mandal, X. De Hatten, B. Baptiste, I. Huc, *Chem. Sci.* **2017**, *8*, 3741–3749; c) P. S. Reddy, B. Langlois d'Estaintot, T. Granier, C. D. Mackereth, L. Fischer, I. Huc, *Chem. Eur. J.* **2019**, *25*, 11042–11047.
[15] a) N. Delsuc, F. Godde, B. Kauffmann, J.-M. Léger, I. Huc, *J. Am. Chem. Soc.* **2007**, *129*, 11348–11349; b) B. t. Baptiste, C. l. Douat-Casassus, K. Laxmi-Reddy, F. d. r. Godde, I. Huc, *J. Org. Chem.* **2010**, *75*, 7175–7185.

[16] a) M. Akazome, Y. Ishii, T. Nireki, K. Ogura, *Tetrahedron Lett.* **2008**, *49*, 4430–4433; b) D. Bindl, E. Heinemann, P. K. Mandal, I. Huc, *Chem. Commun.* **2021**, *57*, 5662–5665.
[17] H. Jiang, J.-M. Léger, I. Huc, *J. Am. Chem. Soc.* **2003**, *125*, 3448–3449.
[18] a) D. Sánchez-García, B. Kauffmann, T. Kawanami, H. Ihara, M. Takafuji, M.-H. I. n. Delville, I. Huc, *J. Am. Chem. Soc.* **2009**, *131*, 8642–8648; b) C. Dolain, J. M. Léger, N. Delsuc, H. Gornitzka, I. Huc, *Proc. Natl. Acad. Sci. USA* **2005**, *102*, 16146–16151; c) M. Vallade, P. Sai Reddy, L. Fischer, I. Huc, *Eur. J. Org. Chem.* **2018**, 5489–5498.
[19] X. Hu, S. J. Dawson, Y. Nagaoka, A. Tanatani, I. Huc, *J. Org. Chem.* **2016**, *81*, 1137–1150.
[20] T. Qi, V. Maurizot, H. Noguchi, T. Charoenraks, B. Kauffmann, M. Takafuji, H. Ihara, I. Huc, *Chem. Commun.* **2012**, *48*, 6337–6339.
[21] C. Dolain, A. Grélard, M. Laguerre, H. Jiang, V. Maurizot, I. Huc, *Chem. Eur. J.* **2005**, *11*, 6135.
[22] R. Wechsel, J. Raftery, D. Cavagnat, G. Guichard, J. Clayden, *Angew. Chem. Int. Ed.* **2016**, *55*, 9657–9661; *Angew. Chem. Int. Ed.* **2016**, *128*, 9809–9813.

Manuscript received: February 18, 2022
Accepted manuscript online: March 25, 2022
Version of record online: April 13, 2022